Spectroscopic analysis of accretion/ejection signatures in the Herbig Ae/Be stars

Tatiana Moura, Silvia H. P. Alencar[1], Alana Paixão de Sousa [2]

[1]Universidade Federal de Minas Gerais - UFMG; [2]Université Grenoble Alpes Grenoble-France

tatiana@fisica.ufmg.br

1 Abstract

We analysed time series of high-resolution UVES/ESO spectra of two Herbig Ae/Be stars, HD 261941 (HAe) and V590 Mon (HBe), that are members of the young (∼ 3 Myr) NGC 2264 stellar cluster and present indications of sufficient circumstellar material for accretion and ejection processes to occur. We determined stellar parameters with synthetic spectral fitting, and studied the variability of emission lines and classified circumstellar lines such as Hα, Hβ, He I λ5875.7, according to their morphologies. We modeled the Hα mean line profile, using a hybrid MHD model that includes a stellar magnetosphere and a disc wind, and find signatures of magnetically driven outflow and accretion in HD 261941, while the Hα line of V590Mon seems to originate predominantly in a disc wind.

2 Selected Stars

- **HD 261941** (CSIMon-000631, Walker 165) is a Herbig Ae star member of the young cluster NGC 2264 and was observed during 21 nights from December 2011 to February 2012 with the UVES (VLT/ESO) spectrograph in the spectral range 4800-6800 Å with resolution of ∼ 47000.
- **V590 Mon** (CSIMon-000392, Lk Hα 25, Walker 90) is a Herbig Be star, also a member of the young cluster NGC 2264 and was observed with the UVES spectrograph during 13 nights from December 2013 to January 2014.

3 Results

Synthetic photospheric spectra were computed using the SME (Valenti et al. 1998) and BinMag4 (Kochukhov 2007) codes, with the ATLAS9 atmosphere models (Kurucz 1993) and a spectral line list from the *Vienna Atomic Line Database* (*VALD*) (Kupka et al. 1999) to determine stellar parameters and obtain the circumstellar spectra contribution. Some parameters results for both stars can be seen in Table 1.

Table 1

Set of parameters of V590 Mon and HD 261941.

Parameter	V590 Mon	HD 261941
M_* [M$_\odot$]	3.2 ± 0.5	$2.32^{+0.20}_{-0.18}$
R_* [R$_\odot$]	2.15 ± 0.20	2.85 ± 0.50
T_{eff} [K]	12500 ± 1500	8500 ± 200
$\log g$	4.5 ± 0.5	3.5 ± 0.5
v_{rad} [km s^{-1}]	40 ± 10	22 ± 2
$v \sin i$ [km s^{-1}]	150 ± 50	120 ± 20
L_{acc} [L$_\odot$]	$7.3^{+2.4}_{-1.8}$	$2.6^{+0.8}_{-0.7}$
R_{cor} [R$_*$]	$1.9^{+1.1}_{-0.5}$	$2.2^{+0.6}_{-0.4}$
$\langle W_{10}(H\alpha)\rangle$ [km s^{-1}]	578 ± 30	537 ± 32
$\dot{M}_{acc}$ [M$_\odot$ yr^{-1}]	$(3.4^{+4.6}_{-1.3}) \times 10^{-7}$	$(2.0^{+1.0}_{-0.7}) \times 10^{-7}$
P [days]	$0.6^{+0.9}_{-0.3}$	$1.2^{+0.9}_{-0.5}$
P$_{max}$ [days]	0.78	1.22
i [°]	∼ 51	∼79

3.1 Circumstellar lines

The best fit photospheric synthetic spectrum was subtracted from the observed spectra to obtain the circumstellar spectra contribution in this system. In Table 1 we list the stellar parameters determined from the spectral line synthesis and the mass accretion rate, obtained from modeling of the Hα circumstellar contribution. The main circumstellar lines are shown in Figs. 3 (HD 261941) and 4 (V590 Mon).

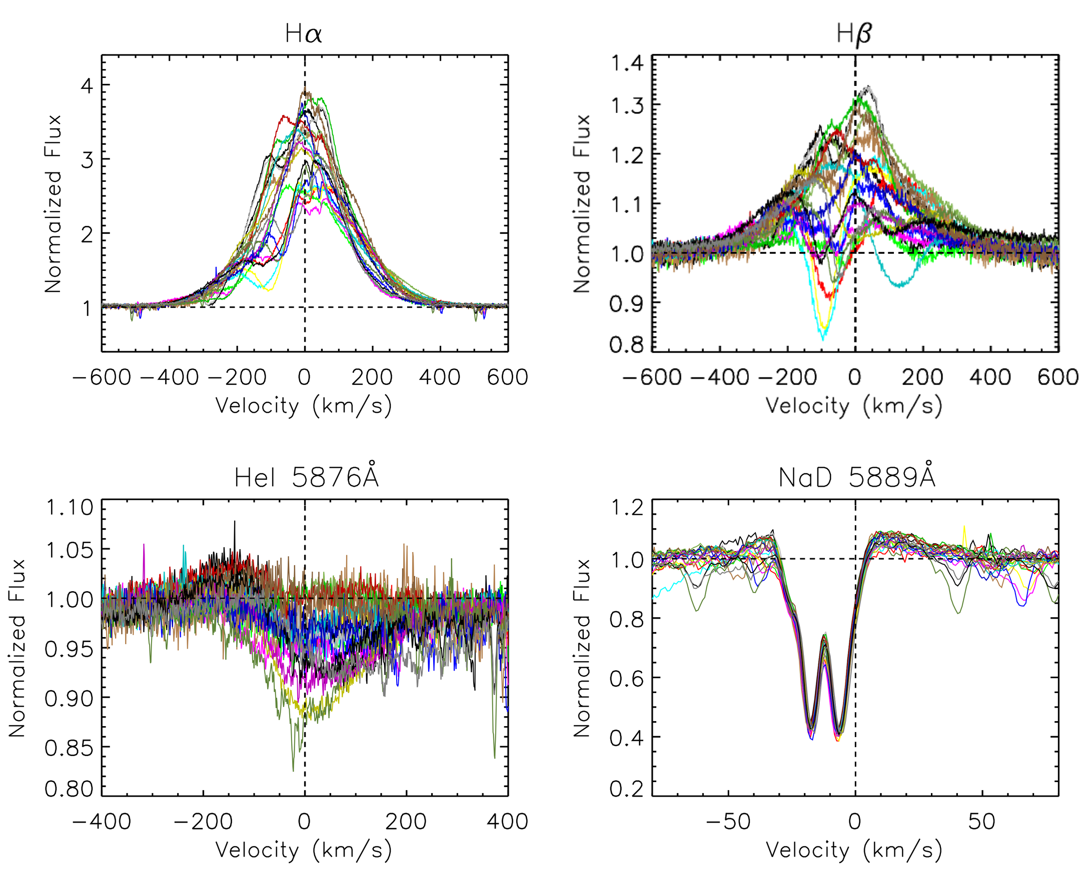

Figure 3. Selected circumstellar spectral lines of HD 261941: Hα, Hβ, He I λ5875.7 and the NaD doublet. The continuum corresponds to the horizontal dashed line and the stellar rest velocity is represented by a vertical dashed line. Each color represents one of the 21 UVES observed spectra.

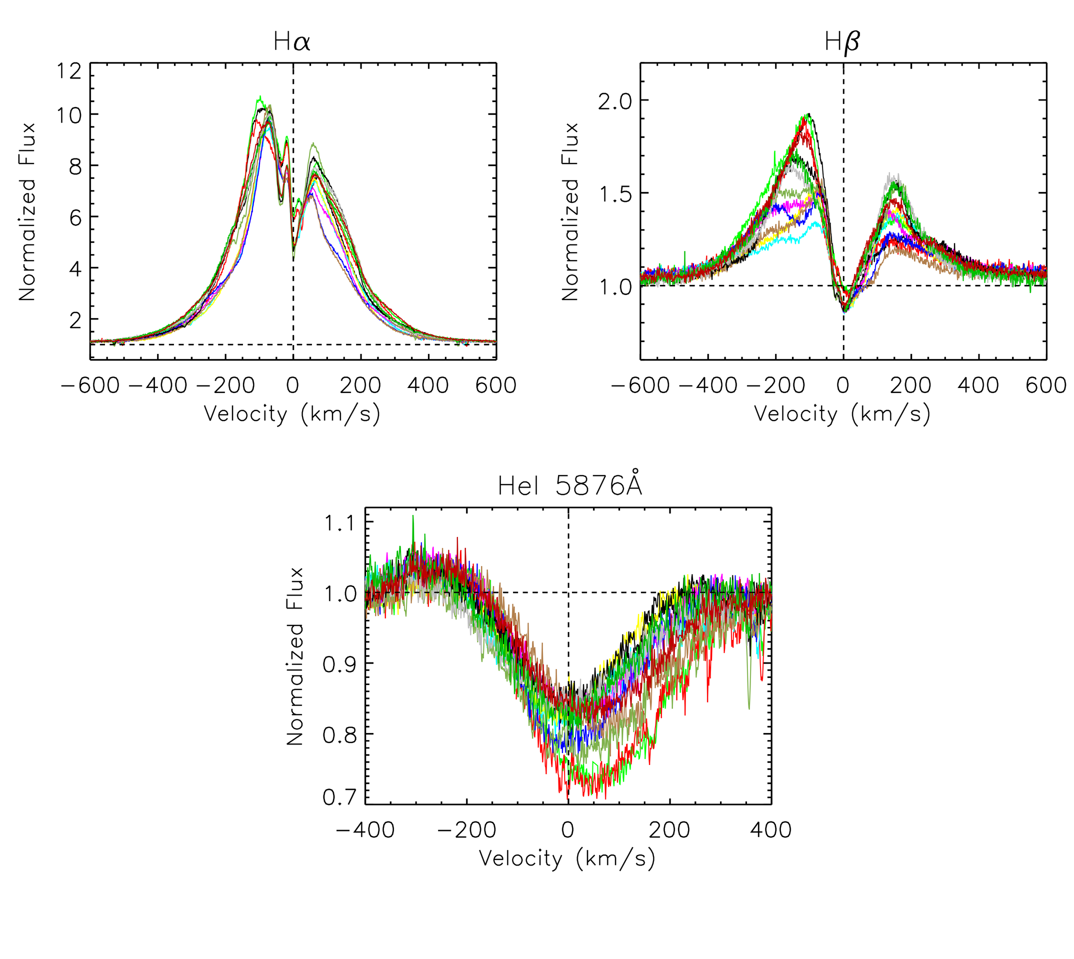

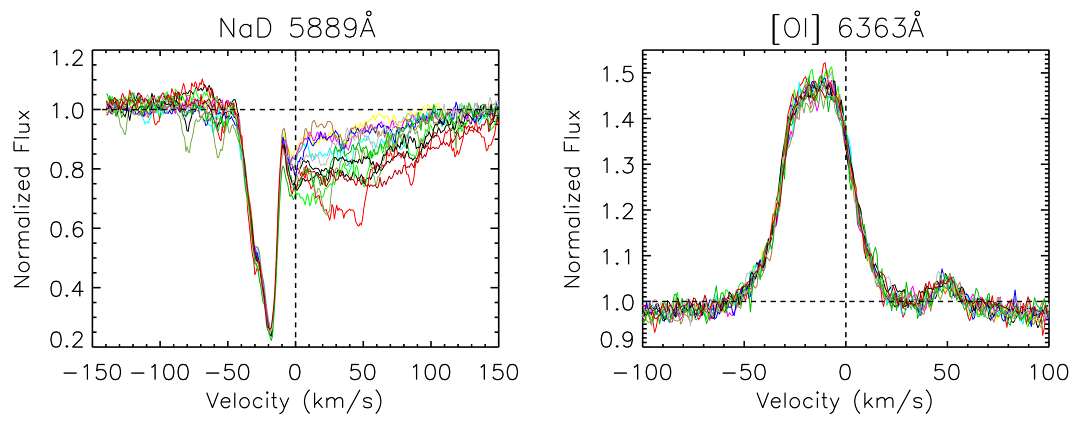

Figure 3. Circumstellar lines of V590 Mon: Hα, Hβ, He I λ5875.7, the NaD doublet and the forbidden oxygen line [OI] λ6363. The continuum corresponds to the horizontal dashed line and the stellar rest velocity is represented by a vertical dashed line. Each color represents one of the 13 observed UVES spectra.

3.2 Morphological classification

We classified the circumstellar lines in groups, as proposed by Cauley & Johns-Krull (2015) as: P-Cygni (PC), inverse P-Cygni (IPC), double-peaked emission (DP), single-peaked emission (E), absorption (A), and featureless (F). The evidence of absorption below the local continuum was classified as PC if the absorption occurs only in the blue side ($v < 0$ km s^{-1}) and as IPC if the absorption occurs only in the red side ($v > 0$ km s^{-1}). Profiles with any other absorption characteristic were classified simply as absorption profile (A). In Fig. 4 we can see some average circumstelar line profiles of V590 Mon.

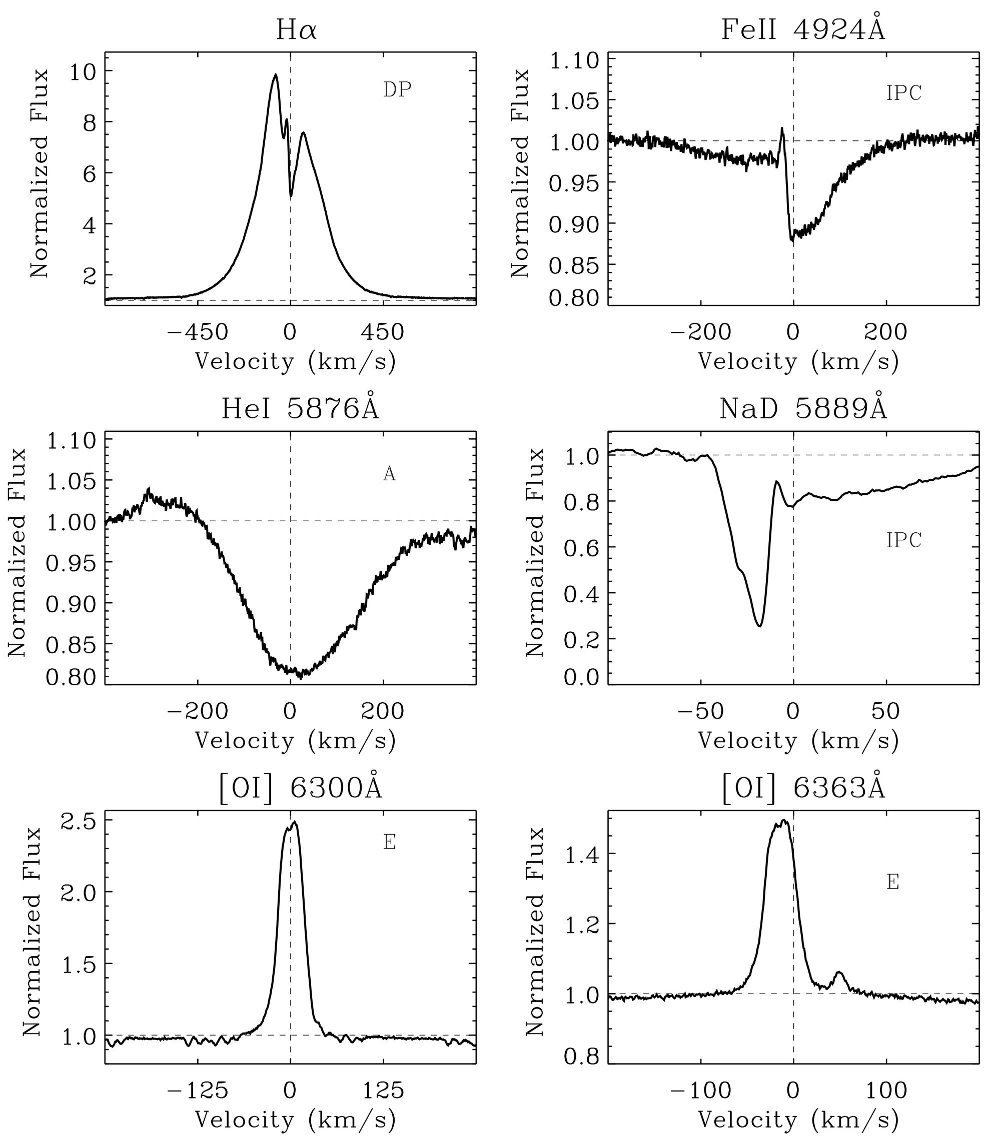

Figure 4. Some average circumstellar line profiles of V590 Mon. The continuum corresponds to the horizontal dashed line and the stellar rest velocity is represented by a vertical dashed line. The profile classification is given on the right upper corner of each plot.

The circumstellar lines of HD 261941 showed a large variability in morphology in our observations. Due to that, we decided to analyse each profile separately, instead of using the mean line profiles (Tab. 2, corresponding to 21 observations of 4 circumstellar lines).

Table 2

Set of parameters of V590 Mon and HD 261941.

Line ID	PC	IPC	DP	E	A	F
Hα	0	0	8	13	0	0
Hβ	3	2	7	6	0	3
HeI λ5876	0	0	0	0	9	12
NaDI λ5889	0	0	0	0	21	0

3.3 Magnetospheric accretion and outflow model

The computational model used in this work was initially proposed by Hartmann et al. (1994) and complemented by Lima et al. (2010). The model allows the calculation of the Hα profile coming from an accreting magnetosphere radiatively coupled to a disc-wind. Figs. 6 (V590 Mon) and 7 (HD 261941) show some results of the Hα line profile modeling and Tables 3 and 4 summarizes the parameters of the best fit models.

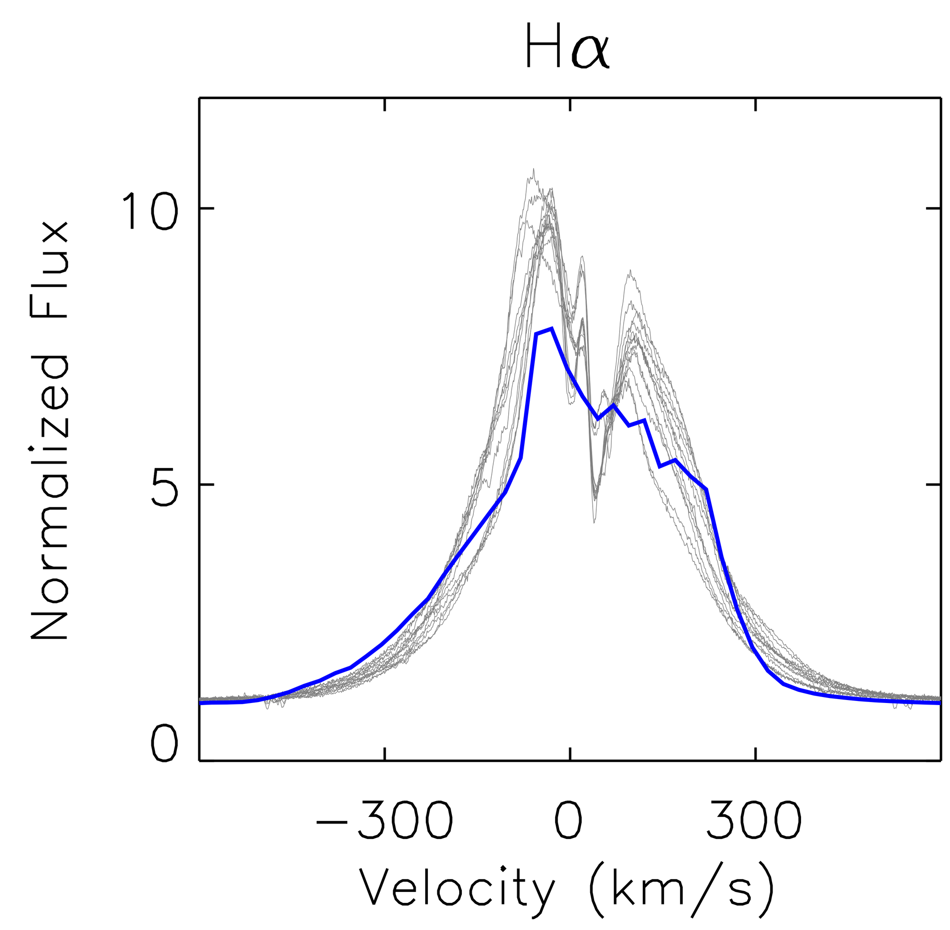

Figure 6. Hα profile of V590 Mon. The observed profiles are shown in grey and the blue lines show the theoretical line profiles from the best model computed with disc-wind component only. The parameters used in the calculations are listed in Tab. 3

Table 3

Disc-wind *CV* models calculated with the stellar parameters of V590 Mon.

Parameters	Values
M_* [M$_\odot$]	3.2
R_* [R$_\odot$]	2.15
i [°]	51
R_{di} [R$_*$]	1.90
R_{do} [R$_*$]	10.00
ϑ_0 [°]	53
ρ [g cm^{-3}]	5.9e-10
T_{wind} [K]	11600
$\dot{M}_{lost}$ [M$_\odot$yr^{-1}]	6.3e-8

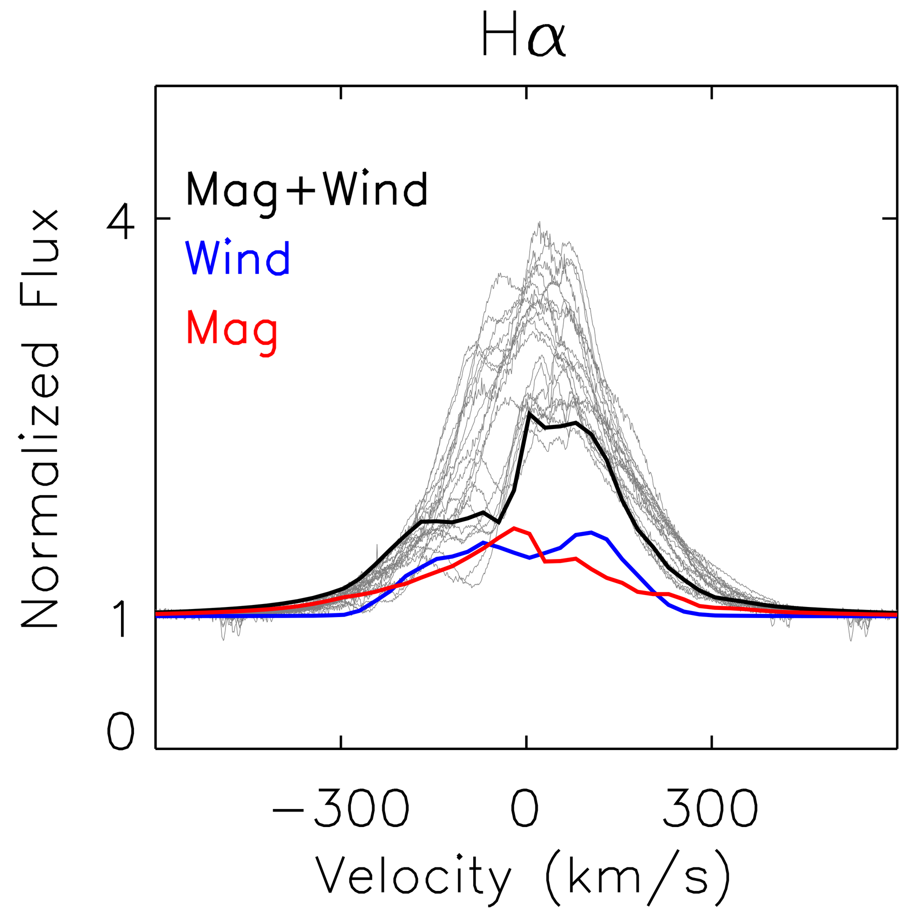

Figure 7. Hα profiles of HD 261941 computed with a hybrid model. The observed profiles are shown in grey. The disc-wind model is represented by a blue line, the magnetospheric contribution is shown as a red line and the resulting hybrid profile is shown in black. The parameters used in the calculations are listed in Tab. 4.

Table 4

Parameters of the best CV model fits of the Hα line of HD 261941 with a hybrid (magnetosphere and disc-wind) model

Parameters	Values
M_* [M$_\odot$]	2.3
R_* [R$_\odot$]	2.9
i [°]	77
R_{mi} [R$_*$]	2.0
R_{mo} [R$_*$]	2.45
R_{di} [R$_*$]	2.50
R_{do} [R$_*$]	10.00
ϑ_0 [°]	31.80
ρ [g cm^{-3}]	1.1e-10
T_{mag} [K]	8200
T_{wind} [K]	8900
$\dot{M}_{acc}$ [M$_\odot$yr^{-1}]	2.8e-7
$\dot{M}_{lost}$ [M$_\odot$yr^{-1}]	2.8e-8

The parameters listed in Tables 3 and 4 correspond to the best fit of the Hα line with the magnetospheric accretion and disc-wind model and are described bellow:

- M_* [M$_\odot$]: Stellar mass;
- R_* [R$_\odot$]: Stellar radius;
- ρ [g cm^{-3}]: Fiducial density;
- ϑ_0 [°]: the disc wind launching angle;
- $\dot{M}_{acc}$ [M$_\odot$yr^{-1}]: the mass accretion rate;
- $\dot{M}_{lost}$ [M$_\odot$yr^{-1}]: the mass loss rate;
- R_{do}: Outer wind radius;
- R_{mi}: Inner magnetosphere radius;
- R_{mo}: Outer magnetosphere radius;
- T_{mag}: Maximum magnetosphere temperature;
- T_{wind}: Maximum disc-wind temperature;
- i: Inclination of the system.

The complet results can be seen in Spectroscopic analysis of accretion/ejection signatures in the Herbig Ae/Be stars HD 261941 and V590 Mon (doi: 10.1093/mnras/staa695)

Acknowledgment

CAPES FAPEMIG CNPq

References

Cauley, P. W. & Johns-Krull, C. M. 2015, ApJ, 810, 5

Hartmann, L., Hewett, R., & Calvet, N. 1994, ApJ, 426, 669

Kochukhov. 2007, Synth3 (Phtsics of Magnetic Stars)

Kupka, F., Piskunov, N., Ryabchikova, T. A., Stempels, H. C., & Weiss, W. W. 1999, A&AS, 138, 119

Kurucz, R. 1993, ATLAS9 Stellar Atmosphere Programs and 2 km/s grid. Kurucz CD-ROM No. 13. Cambridge, Mass.: Smithsonian Astrophysical Observatory, 1993., 13

Lima, G. H. R. A., Alencar, S. H. P., Calvet, N., Hartmann, L., & Muzerolle, J. 2010, aap, 522, A104

Valenti, J. A., Piskunov, N., & Johns-Krull, C. M. 1998, ApJ, 498, 851